E3S Web of Conferences **706**, 02011 (2026) https://doi.org/10.1051/e3sconf/202670602011
INTERCONNECTS 2025

Coefficient of Performance (COP) Analysis on AC Systems Integrated with Water Heater

Muhammad Latifur Rochman[1,2*] and *Muji* Setiyo[1,2]

[1]Department of Mechanical Engineering, Universitas Muhammadiyah Magelang, Magelang, Indonesia
[2]Center of Energy for Society and Industry (CESI), Universitas Muhammadiyah Magelang, Magelang, Indonesia

Abstract. Almost all new vehicles are equipped with an air conditioning system to keep drivers and passengers comfortable. However, the Air Conditioner (AC) system degrades engine performance, increases fuel consumption and emissions, and reduces the range of electric vehicles. During this time, efforts have been made to improve or maintain the performance of AC systems while consuming less power. These efforts continue to focus on enhancing performance. Consequently, this article presents an analysis of the Coefficient of Performance (COP) of a water heating system integrated with an air conditioning system. This water heating system utilizes heat released from the condenser to supply warm water to the bus toilet. Low temperatures and humidity inside buses can decrease passenger comfort, increase the risk of dehydration, and promote the spread of bacteria and germs. According to the study's findings, the lower the mass flow rate of water, the faster the refrigerant's pressure and temperature increase. The findings also emphasize the distinction between COP calculated using an ideal thermodynamic approach and that obtained through experimental methods, which account for losses and inefficiencies.

1 Introduction

Air conditioning (AC) systems play a key role in vehicles by improving comfort and safety for passengers and drivers. They help maintain a pleasant cabin temperature regardless of weather conditions, especially during hot days when interior temperatures can become dangerously high. In addition to temperature control, AC systems also enhance air quality by filtering out dust and pollutants, which helps keep drivers alert and passengers healthy [1,2]. However, running the AC comes at a cost. It draws significant power from the engine or battery, reducing fuel efficiency in traditional cars and cutting the range of electric vehicles by as much as 30–40% [3]. Managing airflow and temperature evenly throughout the cabin can also be difficult due to thermal gradients and interior layout [4]. On top of that, components like compressors and condensers require regular

---

* Corresponding author: latifur@unimma.ac.id

maintenance to keep the system running efficiently [5]. Most vehicle AC systems use a vapor compression cycle, involving four stages—compression, condensation, expansion, and evaporation—outlined in **Fig. 1**, with blue and red indicating low- and high-pressure refrigerant areas.

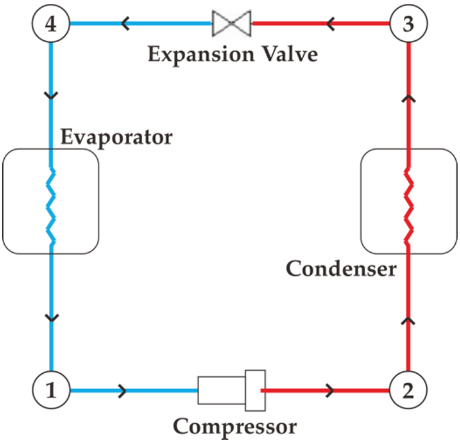

Fig. 1. AC system cycle

Buses introduce additional challenges for AC systems. Because buses are larger and carry more passengers, it's harder to keep the whole cabin at a consistent temperature. This requires larger and more powerful systems, which use more energy and cost more to operate [6]. Frequent stops and open doors also make it difficult to maintain a steady cabin temperature, since cool air escapes quickly [7]. Designing efficient AC systems for buses, therefore, is more complex and remains a pressing concern in the effort to improve comfort and energy efficiency in public transportation.

Some long-distance buses are equipped with toilet facilities, which bring their own set of problems. The limited space often reduces room for passengers and luggage. It's also challenging to keep the toilet area clean, well-ventilated, and at a comfortable temperature. In many cases, the water used in the toilets comes from condensation collected by the AC system's evaporator. While this may seem efficient, the water is often too cold, which can lead to bacteria growth and discomfort for passengers [1,6].

At the same time, there's a large amount of unused heat in the AC system—especially in the condenser, where temperatures can reach up to 61.5 °C. Some studies have looked at using this heat through systems like cascade refrigeration [8] or water spray cooling [9], but these methods are often too complex or require extra equipment. A smarter solution would be to reuse the condenser's waste heat to warm the water for the toilet, especially using heat pump principles [3]. This would let the AC system do two jobs at once: cooling the cabin and heating the water—improving energy use without extra fuel or electricity.

Despite the large amount of recoverable heat from vehicle AC systems, most of it goes unused—especially in buses, where there's a real need for warm water in toilets. This research proposes that an "immersed condenser" design could absorb more heat efficiently, and that this heat can then be reused to warm water for the onboard toilet.

To test this, a modified AC system and measure key performance indicators like temperature, pressure, and Coefficient of Performance (COP) was used. This approach is different from previous studies on cascade systems or external cooling methods [8], because it offers a compact, simpler setup that serves dual purposes without adding significant complexity. The key contribution of this study is to show that we can make AC systems more efficient and multifunctional helping both passenger comfort and sanitation without increasing energy use.

This research aims to evaluate an AC system with an immersed condenser can recover heat and use it to warm water for toilet facilities in buses. Prototype system constructed and tested under controlled laboratory conditions. The study will involve detailed thermodynamic measurements at each stage of the vapor compression cycle, including refrigerant flow, inlet and outlet temperatures, and system pressures. COP will be calculated for both the conventional and modified systems to assess efficiency gains. Additionally, the thermal output of the immersed condenser will be analyzed to determine its effectiveness in meeting the temperature requirements for sanitary water use. This integrated approach is expected to demonstrate a feasible method of enhancing the functionality of vehicle AC systems while supporting broader goals in energy efficiency and sustainable transport technologies.

2 Method

2.1 Set-up experiment

This research uses a small-scale AC system with R134a refrigerant combined with a water heater. During testing, the condenser, which is generally cooled using a fan, was replaced with water cooling, where all parts of the condenser were immersed in water. The water is then circulated with the reservoir via a water pump. **Fig. 2 (a)** shows the experimental set up and location of the pressure (P), temperature (T) and humidity (RH) sensors in this study. **Fig. 2 (b)** shows the Ph-diagram of an AC system. The pressure and temperature of the refrigerant entering the compressor are marked with P_1 and T_1. P_2 and T_2 show the pressure and temperature of the refrigerant entering the condenser. Meanwhile, P_3 and T_3 show the pressure and temperature of the refrigerant entering the expansion valve. Meanwhile, P_4 and T_4 show the pressure and temperature entering the evaporator. To measure the temperature of the water entering and leaving the heat exchanger in the condenser, it is marked with T5 and T6. Humidity and environmental air temperature are indicated by RH7 and T7. The humidity and temperature of the air leaving the evaporator are indicated by RH8 and T8. Temperature was measured using a PT100 3 wire thermocouple, while P_1 and P_4 were measured using PSAN-V01CA-RC1/8 and P_2 and P_3 were measured using TPS20-G33F8-00. Humidity (RH) is measured using a humidity meter. All sensors are connected to the master DAQ as a data logger. The data used during the research were steady data during testing from the 500th to the 3000th seconds. The water mass flow rates used were 0.025, 0.05, 0.075 and 0.1 kg/s.

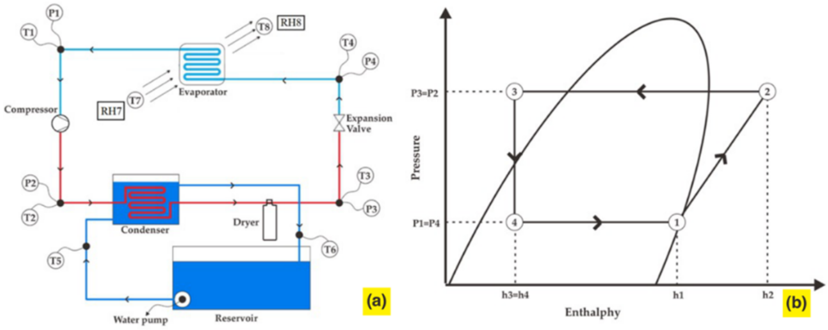

Fig. 2. (a) Set up experiment, (b) Ph diagram

2.2 Analysis method

The COP of the AC system is obtained from the comparison of heat absorption in the evaporation process and compressor power as formulated in Eq. (1).

$$COP = \frac{q_{evap}}{W_{comp}} \tag{1}$$

q_{evap} obtained from Eq. (2):

$$q_{evap} = \dot{m}_r (h_4 - h_1) \tag{2}$$

where, $\dot{m}_r$ = refrigerant mass flow rate; h_4 = Entalphy on point 4 (entering evaporator); h_1 = Entalphy on point 1 (leaving evaporator)

W_{comp} obtained from Eq. (3):

$$W = \dot{m}_r (h_1 - h_2) \tag{3}$$

where, $\dot{m}_r$ = refrigerant mass flow rate; h_1 = Entalphy on point 1 (leaving evaporator); h_2 = Entalphy on point 2 (entering compressor)

Based on Eq. (2) and Eq. (3), obtained Eq. (4).

$$COP = \frac{\dot{m}_r (h_4 - h_1)}{\dot{m}_r (h_1 - h_2)} = \frac{(h_4 - h_1)}{(h_1 - h_2)} \tag{4}$$

In addition, COP can be calculated through the resulting cooling effect compared to the power required for compressor work as formulated in Eq. (5).

$$COP = \frac{Q_{sensible\ air} + Q_{Latent\ condensation}}{W_{comp}} \tag{5}$$

$Q_{sensible\ air}$ obtained from Eq. (6)

$$Q_{sensible\ air} = \dot{m}_{air} . C_{p\ air} . \Delta T \tag{6}$$

where, $\dot{m}_{air}$= air mass flow rate (kg/s); $C_{p\ air}$= specific heat of air (kg/m^3); ΔT= The difference in inlet air temperature (T7) and outlet air temperature (T8)

Air mass flow rate obtained from Eq. (7).

$$\dot{m}_{air} = A_{air}.\rho.V_{air} \quad (7)$$

where, A_{air}= Air cross-sectional area (m^2); ρ= Density of air (kg/m^3); V_{air}= Air velocity (m/s)

$Q_{Latent\ condensation}$ obtained from Eq. (8)

$$Q_{Latent\ condensation} = L_{water}.\dot{m}_{water} \quad (8)$$

where, L_{air}= Heat of evaporation of water (kJ/kg); $\dot{m}_{air}$= Water condensation rate (kg/s)

Meanwhile W_{comp} is obtained from the power needed to drive the compressor, where the compressor driver uses an electric motor as formulated in Eq. (9).

$$W_{comp} = v.I \quad (9)$$

where, v= Motor drive voltage (volt); I= electric current (ampere)

3 Results and discussion

3.1 Assessment of refrigerant pressure and temperature

Fig. 3 shows the pressure and temperature profiles of the refrigerant with water mass flow rates of 0.025, 0.05, 0.075, and 0.1 kg/s. The yellow line shows pressure and temperature at a water mass flow rate of 0.025 kg/s, blue at a water mass flow rate of 0.05 kg/s, black at a water mass flow rate of 0.075 kg/s, while red at a water mass flow rate of 0.1 kg/s. The refrigerant to be compressed is shown in **Fig. 3 (a)**. After passing through the compressor, the pressure and temperature increase **Fig. 3 (b)**. The temperature is then lowered in the condenser **Fig. 3 (c)**, followed by an expansion process to reduce the pressure and a decrease in temperature **Fig. 3 (d)** so that it can be harvested by the evaporator.

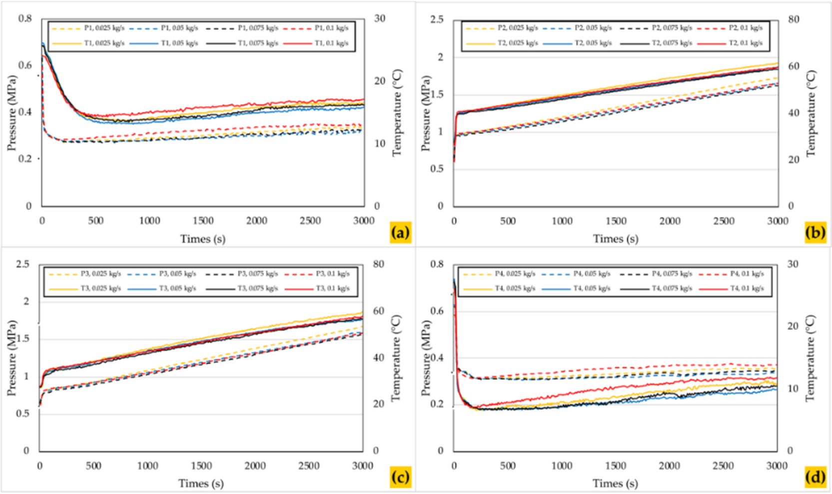

Fig. 3. Refrigerant pressure and temperature profile at: (a) entering compressor; (b) entering condenser; (c) entering expansion valve; (d) entering evaporator

3.2 Assessment of pressure and temperature in the condenser

Fig. 4 shows the pressure and temperature profile in the condenser. The solid line shows the pressure and temperature profile entering the condenser, while the dotted line shows the pressure and temperature leaving the condenser at a water mass flow rate of 0.025, 0.05, 0.075 and 0.1 kg/s are shown in **Fig. 4 (a)** to **Fig. 4 (d)**. Where, the red and blue lines show the pressure and temperature of the refrigerant, and the green colour shows the water temperature. The highest temperature that can be absorbed by water is obtained at a water mass flow rate of 0.025 kg/s with a difference in inlet and outlet water temperatures of 8.88 °C, while the lowest temperature difference is obtained at a water mass flow rate of 0.1 kg/s of 1.36 °C. However, the higher the temperature absorption by water, the faster the change in refrigerant pressure [10]. Where, when the water mass flow rate is 0.25 kg/s it reaches 1.72 MPa while the water mass flow rate is 0.1 kg/s only reaches 1.65 MPa at the same time.

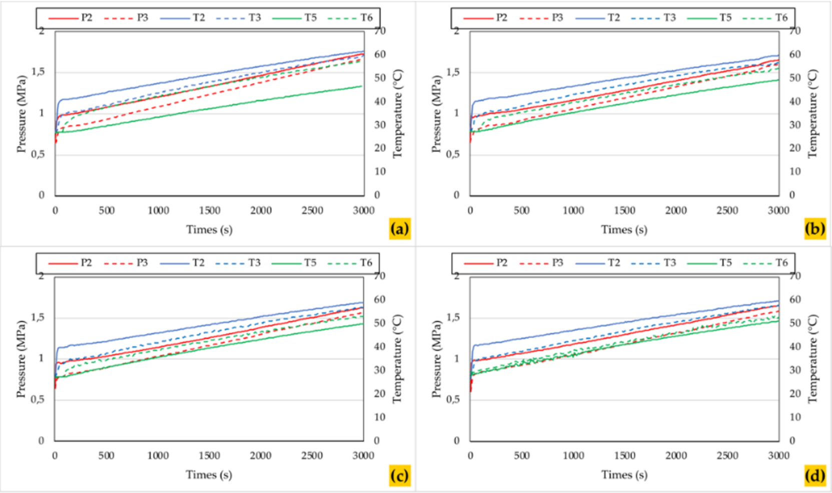

Fig. 4. Pressure and temperature profile in the condenser at water mass flow: (a) 0.025 kg/s; (b) 0.05 kg/s; (c) 0.075 kg/s; (d) 0.1 kg/s

3.3 Assessment of pressure and temperature in the evaporator

Fig. 5 shows the pressure and temperature profile in the evaporator. The solid line shows the pressure and temperature profile entering the evaporator, while the dotted line shows the pressure and temperature leaving the evaporator at a water mass flow rate of 0.025, 0.05, 0.075 and 0.1 kg/s are shown in **Fig. 5 (a)** to **Fig. 5 (d)**. Where, the red and blue lines show the pressure and temperature of the refrigerant, and the green colour shows the air temperature. The lowest air temperature coming out of the evaporator and the average was obtained at a water mass flow rate of 0.05 kg/s, namely 11.8 and 13.4 °C.

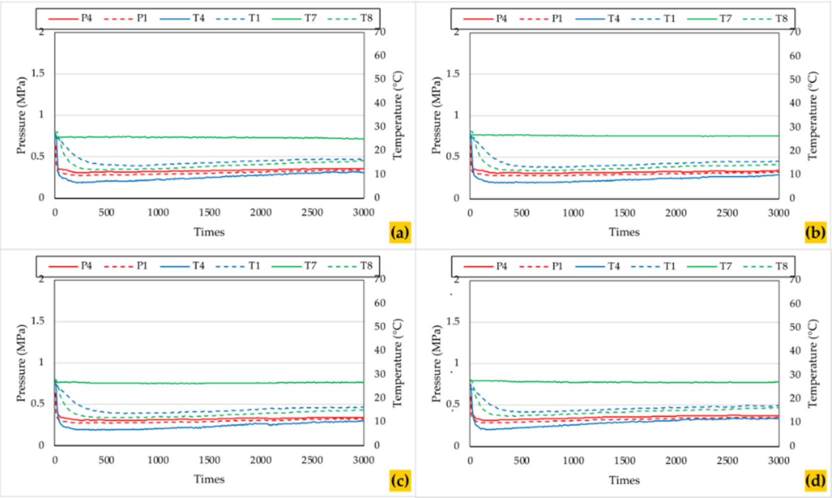

Fig. 5. Pressure and temperature profile in the evaporator at water mass flow: (a) 0.025 kg/s; (b) 0.05 kg/s; (c) 0.075 kg/s; (d) 0.1 kg/s

3.4 COP analysis based on refrigerant pressure and temperature

Based on the pressure and temperature in **Fig. 3**, the enthalpy was calculated using online enthalpy calculator from peacesoftware.de (link). The data used to measure COP used test data at a test time of 500-3000 seconds during steady state conditions and the average enthalpy obtained was as shown in **Table 1**.

Table 1. Enthalpy at various water mass flow rate

Water mass flow (kg/s)	h4	h1	h2
0.025	404	411	427
0.05	404	411	424
0.075	404	411	424
0.1	406	411	424

Based on **Table 1**, the enthalpy is then substituted into Eq. (4) for each water mass flow rate to obtain COP as follows:

Water mass flow 0.025 kg/s:

$$COP = \frac{(h_1 - h_4)}{(h_2 - h_1)} = \frac{(411 - 404)}{(427 - 411)} = 0.44$$

Water mass flow 0.05 kg/s:

$$COP = \frac{(h_1 - h_4)}{(h_2 - h_1)} = \frac{(411 - 404)}{(424 - 411)} = 0.54$$

Water mass flow 0.075 kg/s:

$$COP = \frac{(h_1 - h_4)}{(h_2 - h_1)} = \frac{(411 - 404)}{(424 - 411)} = 0.35$$

Water mass flow 0.1 kg/s:

$$COP = \frac{(h_1 - h_4)}{(h_2 - h_1)} = \frac{(411 - 406)}{(424 - 411)} = 0.38$$

In modern AC systems, generally the COP produced is more than 2 [11]. The change in pressure and enthalpy entering the compressor and condenser increases, this indicates that the refrigerant has been compressed. However, the average difference in temperature between the water and refrigerant leaving the condenser is 2 °C and increases as the water temperature increases (**Fig. 4**). This non-optimal heat release is in line with the temperature of the refrigerant entering the expansion valve which is still high. So, even though the refrigerant has been expanded, the temperature drop only reaches 12.5 °C and the air temperature leaving the evaporator is 9.13 °C. Heat release in the condenser will be more effective when the water used is controlled at a certain temperature. In addition, this study uses an ideal approach and is based on thermodynamic property data, often without considering actual losses such as pressure drop, compressor efficiency, and actual work.

3.5 COP analysis based on cooling effect

Meanwhile the COP obtained based on the cooling effect and electrical power to drive the compressor produced in this research can be calculated using equation (5). Where, the air mass flow rate in the evaporator is 0.465 kg/s with ΔT inlet (T_7) and outlet (T_8) air temperatures is 11.753, 13.447, 13.243 and 12.31 °C, at water mass flow rates of 0.025, 0.05, 0.075 and 0.1 kg/s. Meanwhile, the condensation rate is 0.00019, 0.00018, 0.00022 and 0.00025 at water mass flow rates of 0.025, 0.05, 0.075 and 0.1 kg/s. The compressor is driven using an electric dynamo with an electric current of 7 amperes and a voltage of 220 volts to obtain the following **Table 2**.

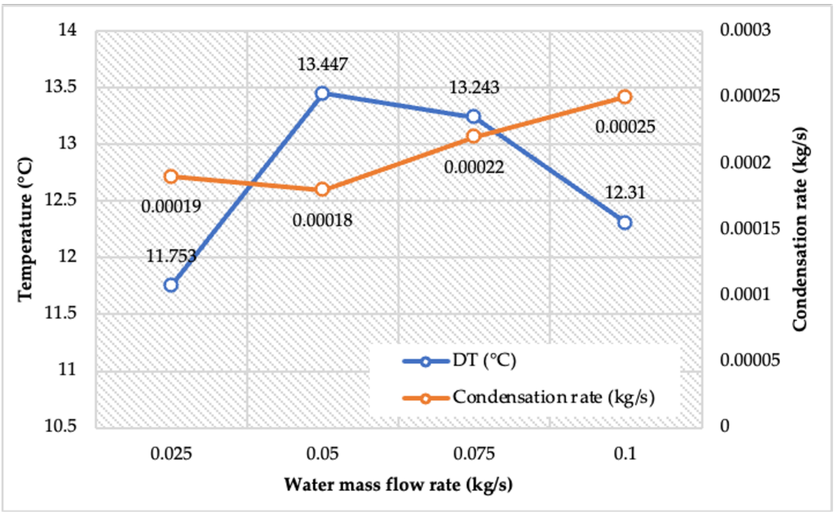

Fig. 6. Average difference inlet (T7) and outlet (T8) air temperature and condensation rate

Table 2. COP based on cooling effect at various water mass flow rate

Water mass flow (kg/s)	Qsensible air	Qlatent condensation	Wcomp	COP
0.025	0.549	0.419	1.386	0.698
0.05	0.628	0.416	1.386	0.753
0.075	0.618	0.502	1.386	0.808
0.1	0.575	0.555	1.386	0.815

The test results showed that the temperature difference between the inlet (T7) and outlet (T8) water (**Fig. 6**), denoted as ΔT, followed a parabolic pattern. At a water mass flow rate of 0.025 kg/s, the ΔT reached a peak of 11.753 °C. This occurs because lower flow rates allow more time for heat absorption, resulting in a faster increase in reservoir water temperature, which is consistent with previous findings [12]. In contrast, at higher flow rates ranging from 0.05 to 0.1 kg/s, ΔT gradually decreased. This reduction is likely due to increased desorption and reduced heat exchange time, as the water moves more quickly through the system.

The COP produced is less than 1, this can be influenced by the magnitude of the electric current, which is not measured in real time, along with a decrease in the ability to release heat in the condenser which is in line with the increase in compressor work. In addition, this research uses an experimental or practical approach and may include actual losses such as: mechanical friction; incomplete heat transfer; heat transfer to the environment; electrical energy for fans or other sensors [13].

This research can be applied to buses that have toilets to increase comfort [14] and reduce the risk of dehydration due to low humidity on buses [15]. However, a review needs to be carried out regarding the water temperature needed to keep the air temperature in the cabin low. As well as measuring compressor work in real time to obtain more precise COP calculations.

4 Conclusion

Study related to harvesting condenser temperatures using water has been carried out. The findings also emphasize the distinction between COP calculated using an ideal thermodynamic approach and that obtained through experimental methods, which account for losses and inefficiencies. The results show that the lower the water mass flow rate is in line with the faster increase in refrigerant pressure and temperature at the same time. The COP calculated based on the ideal thermodynamic approach and experimental methods is 0.44, 0.54, 0.35, and 0.38 and 0.698, 0.753, 0.808, 0.815 at a water mass flow rate of 0.025, 0.05, 0.075, and 0.1 kg/s.

References

1. Guo, R.; Zhu, X.; Zhu, Z.; Sun, J.; Li, Y.; Hu, W.; Tang, S. Evaluation of Typical Volatile Organic Compounds Levels in New Vehicles Under Static and Driving Conditions. *Int. J. Environ. Res. Public Health* **2022**, *19*, 7048, doi:10.3390/ijerph19127048.
2. Abam, F.I.; Ndukwu, M.C.; Inah, O.I.; Uchechukwu, O.D.; Setiyo, M.; Samuel, O.D.; Uche, R. Thermodynamic Modelling of a Novel Solar-ORC with Bottoming Ammonia-Water Absorption Cycle (SORCAS) Powered by a Vapour Compression Refrigeration Condensate for Combined Cooling and Power. *Mech. Eng. Soc. Ind.* **2023**, *3*, doi:10.31603/mesi.10365.
3. Xi, L.; Wang, L.; Zhao, C.; Luo, X.; Feng, B. Research on Fuzzy Control Strategy of Heating Condition Based on Electric Vehicle Heat Pump Air Conditioner. *Acad. J. Sci. Technol.* **2022**, *3*, 175–181, doi:10.54097/ajst.v3i3.2932.
4. Lesage, M.; Chalet, D.; Migaud, J.; Krautner, C. Holistic Approach to Improve Cabin Air Quality in Electric Vehicles and Energy Savings. In Proceedings of the 36th International Conference on Efficiency, Cost, Optimization, Simulation and Environmental Impact of Energy Systems (ECOS 2023); ECOS 2023: Las Palmas

De Gran Canaria, Spain, 2023; pp. 2402–2413.

5. Sukarno, R.; Rafael, M.; Yoga, N.G.; Syaka, D.R.B.; Permana, A.A.; Gunawan, Y.; Kurniawati, D. Innovative Pickup Car Cooling System Based on Thermoelectric Coupled With Heat Pipe Sink. *Automot. Exp.* **2025**, *8*, 296–309, doi:10.31603/ae.13494.
6. Rusdjijati, R.; Purnomo, B.C.; Rochman, M.L.; Pertiwi, F.D.; Setiyo, M. Integration of Water Heating Systems with Car Air Conditioning Systems: A Bibliometric Analysis, Lab-Scale Investigation, and Potential Applications. *Indones. J. Sci. Technol.* **2025**, *10*, 75–92, doi:10.17509/ijost.v10i1.80966.
7. Liang-hong, Z.; Hou, W.; He, Q. Intelligent of Electric Vehicle Heat Pump Air Conditioning Control System. *J. Phys. Conf. Ser.* **2021**, *2143*, 12043, doi:10.1088/1742-6596/2143/1/012043.
8. Li, D.; Bai, T.; Yu, J. Thermodynamic Performance Optimization and Analysis of an Auto-Cascade Refrigeration Cycle with Vapor Injection for Ultra-Low Temperature Freezer. *Int. J. Refrig.* **2023**, *145*, 425–435.
9. Sukri, M.F.; Lokman, R.; Muhajir, A.; Wasbari, F.; Damanhuri, A.A.M.; Sumeru, K. The Effect of Condensate Water on the Performance of Automotive Air Conditioning System under Difference Evaporator Air Inlet Temperature. *Int. J. Nanoelectron. Mater.* **2020**, *13*, 85–94.
10. Orodu, K.B.; Okoro, E.E.; Ijalaye, O.K.; Orodu, O.D. Gas Compressibility Factor Explicit Correlations for Range of Pseudo Reduced Temperature and Pressure. *Flow Meas. Instrum.* **2019**, *67*, 176–185.
11. Borikar, S.A.; Borikar, D.A.; Panchal, H.; Cuce, E.; Dalkilic, A.S.; Alrubaie, A.J.; Jaber, M.M. An Experimental Case Study on the Effect of Condenser Geometry in a Refrigerator: Sub-Cooling and Coefficient of Performance Issues. *Int. J. Refrig.* **2023**, *148*, 75–82, doi:10.1016/j.ijrefrig.2023.01.002.
12. Ibarra-Bahena, J.; Rivera, W.; Nanco-Mejía, S.D.; Romero, R.J.; Venegas-Reyes, E.; Dehesa-Carrasco, U. Experimental Performance of a Membrane Desorber Operating under Simulated Warm Weather Condensation Temperatures. *Membranes (Basel).* **2021**, *11*, 474, doi:10.3390/membranes11070474.
13. Al doori, W.H. The Effects of Nusselt, Reynolds Number, and Pressure Drop on the Thermal Performance of Pierced Pin Fins. *Front. Heat Mass Transf.* **2022**, *19*, 1–9, doi:10.5098/hmt.19.8.
14. Setiyo, M.; Waluyo, B.; Widodo, N.; Rochman, M.L.; Munahar, S.; Fatmaryanti, S.D. Cooling Effect and Heat Index (HI) Assessment on Car Cabin Cooler Powered by Solar Panel in Parked Car. *Case Stud. Therm. Eng.* **2021**, *28*, 101386, doi:10.1016/j.csite.2021.101386.
15. Jones, M.D.; Hooton, J.C.; Dawson, M.L.; Ferrie, A.R.; Price, R. Dehydration of Trehalose Dihydrate at Low Relative Humidity and Ambient Temperature. *Int. J. Pharm.* **2006**, *313*, 87–98.